A COMPARISON STUDY OF THE EFFECTIVENESS OF THREE VENTILATION SYSTEMS IN PURGING POLLUTANT USING CFD

G. H. Yeoh and Y. Li

Advanced Thermo-fluids Technologies Laboratory
CSIRO, Division of Building, Construction & Engineering, AUST[illegible]

ABSTRACT

A three-dimensional mathematical model to solve the mixing, displacement and vortex ventilation systems in the removal of pollutants with a thermal source is described. The study carried out to investigate the effectiveness of each of the individual ventilation systems showed that the vortex ventilation system performed better than the other two systems in providing moderate occupancy thermal comfort but very effective in purging pollutants away from a typical office room environment.

KEYWORDS

Air quality, CFD, displacement ventilation, mixing ventilation, vortex ventilation

INTRODUCTION

The flow characteristics within a building or individual zones or rooms can have a considerable impact on ventilation energy performance. Indoor airquality represents one of the many issues in ventilation technologies where pollutants are present. It is well-known that the presence of heat sources in building environments will significantly influence the propagation of the airborne pollutants. Primary air streams such as jets and gravity currents interact with the plumes generated above the heat sources. The ventilation effectiveness of resulted airflow pattern often depends on how the air distribution method utilises the interaction between the primary air streams and thermal plumes. The study of different ventilation strategies in purging pollutants is therefore important. Such investigation would comprise of evaluating the performance of these ventilation systems and determining the degree of success of the purging process. This comparison study will lead to ascertaining the most optimal design for ventilation effectiveness and general comfort of occupants.

In this paper, three ventilation systems will be investigated - mixing, displacement and vortex.

The various aspects of the mathematical formulation employing the Computational Fluid Dynamics (CFD) techniques to predict the transient development of the mixing of air and pollutants in a room are provided. A three-dimensional (3-D) simulation is carried out. A finite volume approach is employed to discretise the time-averaged conservation equations. Efficient solution techniques are used to solve the incompressible time-averaged equations of motion and energy governing the turbulent airflow. The velocity-pressure linkage is handled via the SIMPLEC (Van Doormal and Raithby 1984) algorithm. The present model invokes the Boussinesq approximation to simplify the calculations and adopts a RNG κ-ε turbulence model. The pollutant is solved as a passive scalar. Computed results for the development of the mixing process through time are shown. Recommendations and possible directions for practical design of ventilation systems are discussed.

MODEL ROOMS ANALYSED

Figures 1 (a) - (c) show the configuration of the analysed model rooms for the mixing, displacement and vortex ventilation systems respectively. Each of these rooms has dimensions of 4.2 × 3.6 × 2.5 m, representing a typical office room. The heat source was located at the centre in each of the rooms with a size of 0.5 × 0.3 × 0.4 m. The pollutants were taken to originate from the heat source. It was assumed that the pollutants were passive, particle loss due to aggregation and deposition, change in particle size distribution and gravity sedimentation are neglected. For the cases of the mixing and displacement ventilation systems, only half the room was modelled because of symmetry.

The air flow rate $\dot{V}$ for each of the three systems was set at 189 m^3/h or 0.0525 m^3/s, which is 5 air change per hour (ACH) for the room. The different sizes of the supply outlet and exhaust inlet for the three systems and the supply air temperatures are tabulated in Table 1.

In all the numerical calculations, the density ρ and specific heat C_p have been taken to have values of 1.29 kg/m^3 and 1000 J/kgK. By assuming that the temperature difference ΔT between the exhaust inlet and supply outlet to be 6 K, the capacity of the heat source can be determined from: $\dot{Q} = \rho C_p \dot{V} \Delta T$ (noting that the air flow rate $\dot{V}$ is given from above) - a value of 406.25 W is obtained.

A total mesh size of 21252 grid points was generated for the mixing ventilation, 26312 grid points for the displacement ventilation and 24840 grid points for the vortex ventilation.

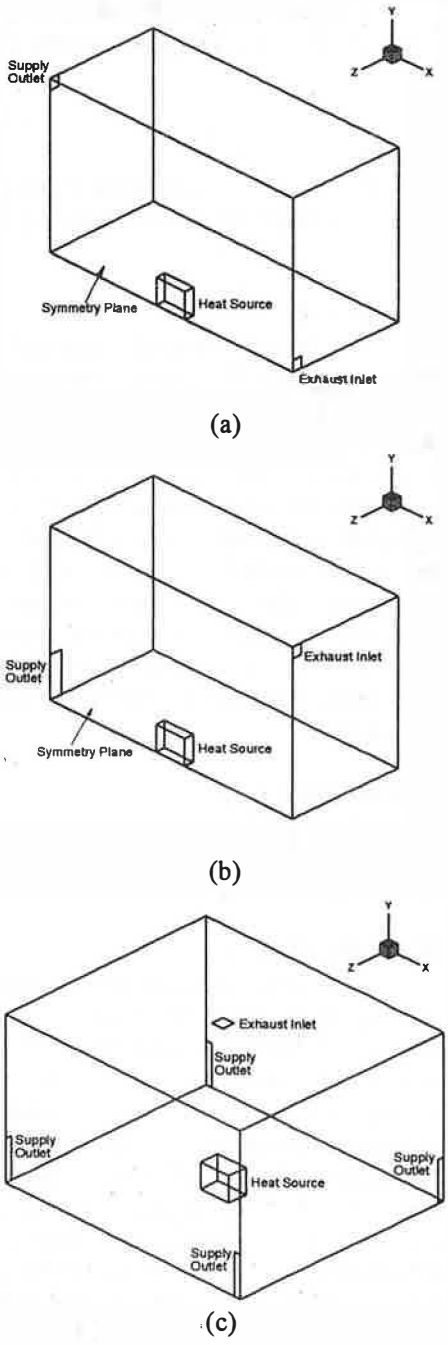

Figure 1 Schematic representation of the model analysed for: (a) Mixing Ventilation, (b) Displacement Ventilation and (c) Vortex Ventilation systems.

Table 1 Configuration details for the Mixing, Displacement and Vortex Ventilation systems.

	Supply Air velocity	Supply Outlet Size	Exhaust Inlet Size	Inlet Temperature
Mixing	1 m/s	0.3 × 0.175 m	0.3 × 0.175 m	288.15 K
Displacement	0.2 m/s	0.65625 × 0.4 m	0.3 × 0.175 m	291.15 K
Vortex	0.2 m/s	0.1 × 0.65625 m	0.2 × 0.2 m	291.15 K

MATHEMATICAL FORMULATION

Governing equations

The fluid flow, heat transfer and the distribution of pollutants in the enclosure space were described by the three-dimensional, time-averaged equations of transport for mass, momentum, energy and a passive scalar.

The velocities along the Cartesian x, y and z directions are denoted by u, v, and w respectively.

Turbulence is modelled using the Renormalization-Group (RNG)-based κ-ε model (Yakhot and Orszag 1992). The empirical constants are set to C_μ = 0.085, C_1 = 1.42, C_2 = 1.68, C_3 = 1.44, σ_κ = 0.7179, σ_ε = 0.7179. The RNG theory leads to a differential relation for the eddy viscosity ν_{eddy} which after integration yields a simplified algebraic form valid from high to low Re (Orszag et. al. 1993):

$$\nu_t = \nu_{eddy} - \nu_o$$

$$\nu_{eddy} = \nu_o \left[1 + \sqrt{\frac{C_\mu}{\nu_o}} \frac{\kappa}{\sqrt{\varepsilon}} \right]^2 \qquad (1)$$

where ν_o = dynamic viscosity
ν_t = turbulent viscosity

The RNG κ-ε model also possesses the capability to accommodate high strain rates via the derivation of an additional term, R, namely,

$$R = \frac{C_\mu \eta^3 (1 - \eta/\eta_o)}{1 + \beta \eta^3} \frac{\varepsilon^2}{\kappa},$$

$$\eta = \frac{P\kappa}{\varepsilon}, \eta_o = 4.38, \beta = 0.012, \qquad (2)$$

$$P = \nu_t \left(\frac{\partial u_i}{\partial x_j} + \frac{\partial u_j}{\partial x_i} \right)^2$$

In the κ and ε equations, the production of turbulence due to buoyancy and the effect of thermal stratification on the turbulence dissipation rate are included by the term, G, *viz.*,

$$G = g\beta_{ref} \frac{\nu_t}{\sigma_t} \frac{\partial T}{\partial y} \qquad (3)$$

where $\beta_{ref} = 1/T_{ref}$
T_{ref} = reference temperature

The reference temperature was taken to be at the supply air temperature.

For the thermal calculation, a volumetric heat source was embedded as a source term in the temperature equation. Within this specified volume, the relative value of the pollutants was set to be 1.

The conservation equations were cast in the following form:

$$\frac{\partial \phi}{\partial t} + \nabla \cdot (\bar{u}\phi) = \nabla \cdot (\Gamma_\phi \nabla \phi) + S_\phi \qquad (4)$$

The variables, together with the exchange coefficients and source terms, are given in Table 2.

The effective Prandtl number σ_t and Schmidt number σ_p (Table 1) for the temperature T and the pollutant Y_p are assumed to have the values of 0.7.

Boundary conditions

Standard wall functions were used for the enclosure walls. On the symmetry plane, zero Neumann conditions for all variables except for the w velocity along the

Table 2 Transport equations for variable ϕ in the flow field.

ϕ	Γ_ϕ	S_ϕ
1	0	0
u	ν_{eddy}	$-\frac{1}{\rho}\frac{\partial p}{\partial x}+\frac{\partial}{\partial x}\left(\nu_{eddy}\frac{\partial u}{\partial x}\right)+\frac{\partial}{\partial y}\left(\nu_{eddy}\frac{\partial v}{\partial x}\right)+\frac{\partial}{\partial z}\left(\nu_{eddy}\frac{\partial w}{\partial x}\right)$
v	ν_{eddy}	$-\frac{1}{\rho}\frac{\partial p}{\partial y}+\frac{\partial}{\partial x}\left(\nu_{eddy}\frac{\partial u}{\partial y}\right)+\frac{\partial}{\partial y}\left(\nu_{eddy}\frac{\partial v}{\partial y}\right)+\frac{\partial}{\partial z}\left(\nu_{eddy}\frac{\partial w}{\partial y}\right)-g\beta_{ref}\left(T-T_{ref}\right)$
w	ν_{eddy}	$-\frac{1}{\rho}\frac{\partial p}{\partial z}+\frac{\partial}{\partial x}\left(\nu_{eddy}\frac{\partial u}{\partial z}\right)+\frac{\partial}{\partial y}\left(\nu_{eddy}\frac{\partial v}{\partial z}\right)+\frac{\partial}{\partial z}\left(\nu_{eddy}\frac{\partial w}{\partial z}\right)$
κ	$\frac{\nu_{eddy}}{\sigma_\kappa}$	$P+G-\varepsilon$
ε	$\frac{\nu_{eddy}}{\sigma_\varepsilon}$	$\frac{\varepsilon}{\kappa}c_1P+\frac{\varepsilon}{\kappa}c_3\max(G,0)-R-c_2\frac{\varepsilon^2}{\kappa}$
T	$\frac{\nu_{eddy}}{\sigma_t}$	$\frac{\dot{Q}}{\rho_{ref}C_p}$
Y_p	$\frac{\nu_{eddy}}{\sigma_p}$	0

Cartesian z direction was set to zero. Across the exhaust inlet, zero Neumann conditions were imposed for all variables. In order to satisfy overall conservation of mass, the velocity components were extrapolated from upstream nodal points and then adjusted to the desired air flow rates. At the supply outlet, a constant mass flux is applied. Turbulence of kinetic energy κ is calculated from $0.002\,u_{in}$ where u_{in} is the velocity determined from the mass flux, while the dissipation rate ε is determined through $\kappa^{3/2}/l_\varepsilon$ where l_ε is the hydraulic diameter of the supply outlet

For the mixing and vortex ventilation systems, adiabatic condition for the temperature was applied at the enclosure walls. Boundary temperatures for the displacement ventilation system were, however, calculated from algebraic expressions and specified as input to the numerical simulation. This is to account for the radiative heat transfer between room surfaces, particularly between the ceiling and the floor. A simple displacement ventilation model (Li et al. 1992) was used to determine the temperatures at the ceiling and the floor. It solves two algebraic expressions in relation to the supply outlet and exhaust inlet temperatures. The equations are:

$$\begin{aligned} T_{floor}-T_{supply} &= T_{exhaust}-T_{ceiling} \\ T_{ceiling}-T_{floor} &= 0.6(T_{exhaust}-T_{supply}) \end{aligned} \quad (5)$$

Since the supply outlet and exhaust inlet temperatures are known, using equation (5), the ceiling and floor temperatures were evaluated to be 295.95 K and 292.35 K respectively. The boundary temperatures at the rest of the room surfaces were taken as the average of the ceiling and floor temperatures, ie. 294.15 K.

SOLUTION PROCEDURE

The time derivative for each of the equations was approximated using the first-order forward difference scheme. The diffusion terms and other gradients were discretized using the second-order central difference approximation. The first-order hybrid (upwind/central) scheme was employed for the convective terms.

The set of equations of the field variables ϕ was solved implicitly using the Strongly Implicit Procedure (SIP) (Stone, 1968).

A time step of 1 second was employed for the computational calculations. At any time step, the solution was considered converged if

$$\frac{\left|\phi^{n+1}(i,j,k)-\phi^{n}(i,j,k)\right|}{\max\left|\phi^{n+1}(i,j,k)\right|} < 10^{-3} \quad (6)$$

where n = iteration loop counter.

RESULTS AND DISCUSSION

The effective operation of the mixing, displacement and vortex ventilation systems were investigated by the consideration of issues in regards to thermal comfort and the effective purging of the pollutants. Computational results for these issues are represented by contour plots of T and Y_p. The transient time of these plots was taken at 30 min.

At the time of 30 min, the numerical simulation revealed that the flow and heat transfer characteristics and their effect on the pollutants distribution for the mixing and displacement ventilation systems have almost reached a steady state behaviour but not for the vortex ventilation system. It is currently not known whether the case of the vortex ventilation system required a longer time to reach a steady state situation or the system may have a periodic behaviour in time. Further investigations would be carried out to probe into the physical phenomena of the complex flow and heat transfer of the vortex ventilation system.

The thermal comfort of the enclosure model analysed for the three systems are shown by the temperature distribution at symmetry plane for the mixing and displacement ventilation systems and midway along the z-direction for the vortex ventilation system in Figures 2 (a) - (c). It is clearly seen that the mixing ventilation system provides a rather uniform indoor air temperature distribution as expected. The vortex ventilation system, however, responded better in restricting the hot layer towards the ceiling of the enclosure than the displacement ventilation system.

The purging of pollutants for the three systems illustrated by the passive scalar distribution at the same location of the temperature distribution can be seen in Figures 3 (a) - (c). Here, the vortex ventilation system seemed to outperform the mixing and displacement ventilation systems in the purging process of pollutants. This behaviour could be explained by the fact of an adherent vorticity that was introduced by the nature of flow phenomenon which enabled it to provide a swirling action in lifting the pollutants above the heat source and contained them in the temperature hot layer. This is beneficial for occupancy health as the heavy concentration of pollutants stayed above the height of the occupants.

Figures 4 (a) and (b) show the velocity vectors of the flow characteristics for the mixing and displacement systems at the symmetry plane. For the mixing ventilation system, the origin of the

buoyancy force at the heat source was effectively suppressed and has no effect on the overall flow behaviour. This is because of the penetration of the large entrainment from the supply outlet into the heat source regions at a much greater force than the action of the buoyancy force. Nevertheless, the displacement ventilation system uses the effect of buoyancy as part of the design configuration and the intense velocities around the heat source succinctly illustrated the strong buoyancy force lifting the flow up towards the ceiling.

Figures 5 (a) - (c) illustrate the complex flow behaviour of the vortex ventilation system. Figure 5 (a) indicates the velocity vectors seen from the plan view just above the floor level; Figure 5 (b) shows the plan view of the flow just below the ceiling level; and Figure 5 (c) demonstrates the flow behaviour cutting through the heat source at the midway along the x-direction. It is noted that the flow seen at the floor level was slightly displaced from the centre of the heat source. This behaviour could be due to the competing actions between the buoyancy force and shear force acting concurrently through time. These three figures clearly illustrate the interesting flow phenomenon of the vortex ventilation systems in regards to the swirling action of the flow taking place as the progressment of the flow was seen stepping up from the floor to ceiling levels.

CONCLUSION

The development of a numerical model to handle the three ventilation systems - mixing, displacement and vortex - in purging pollutants with the effect of a thermal source was formulated. The effectiveness of these three systems considering occupancy thermal comfort and their ability to successfully remove pollutants away from the enclosure space was evaluated in a preliminary comparison study. The results were:

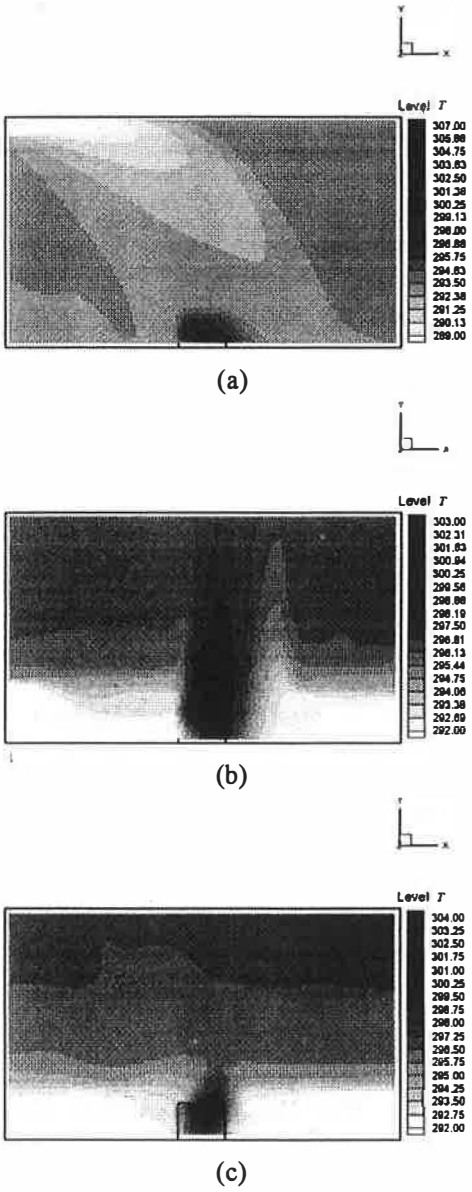

Figure 2 Temperature contours at 30 min for (a) Mixing Ventilation, (b) Displacement and (c) Vortex Ventilation systems.

1) As expected, the mixing system provides a rather uniform environment for both temperature and pollutant concentration, while both displacement and vortex systems provide a flow pattern with both thermal and

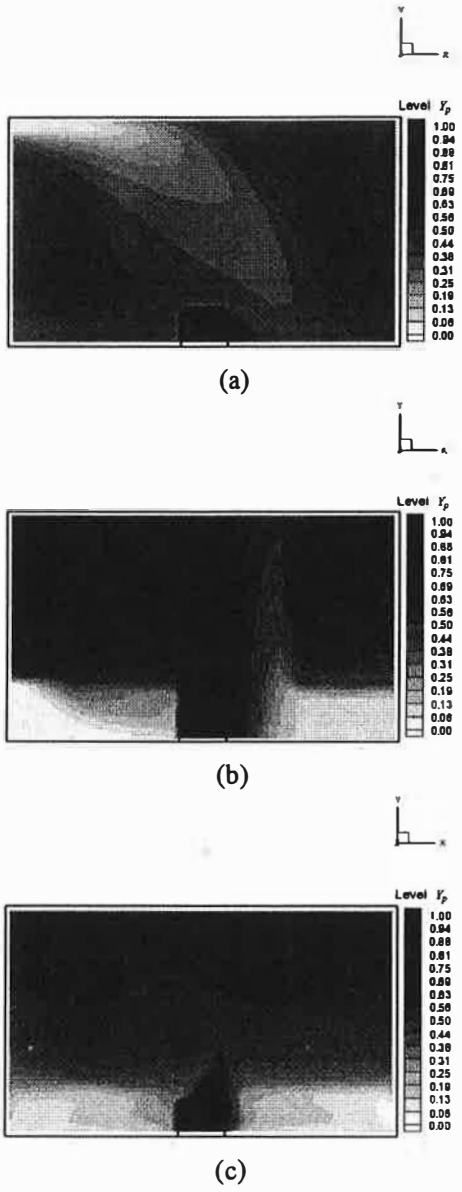

Figure 3 Pollutants contours at 30 min for (a) Mixing Ventilation, (b) Displacement and (c) Vortex Ventilation systems.

concentration stratification.

2) The vortex system seems to be the most effective system in the removal of pollutants. This is possibly due to the fact that both thermal plumes and swirling flows are utilised to provide upward flows. However, there seems to be certain air flow instability in the vortex ventilation system. Effectively, the vortex ventilation studied in this paper is a swirling-flow-assisted displacement system as low air velocity supply is used.

It is therefore recommendable to consider the vortex ventilation system as a practical ventilation system for design engineering purposes in some applications..

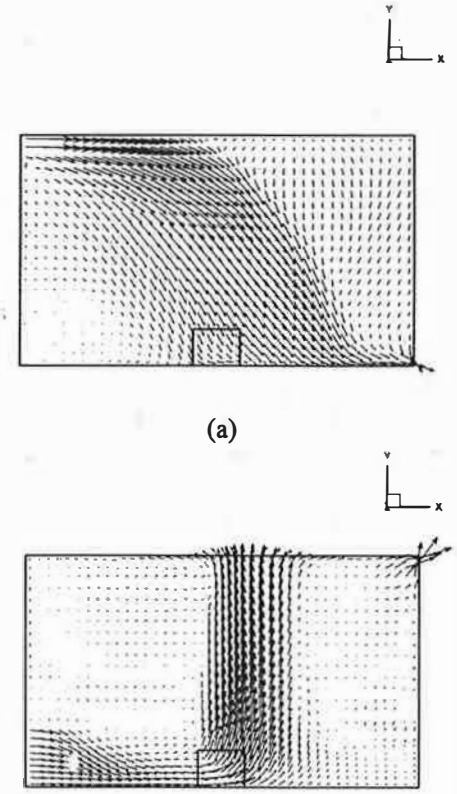

Figure 4 Velocity vectors at 30 min for: (a) Mixing Ventilation and (b) Displacement Ventilation systems

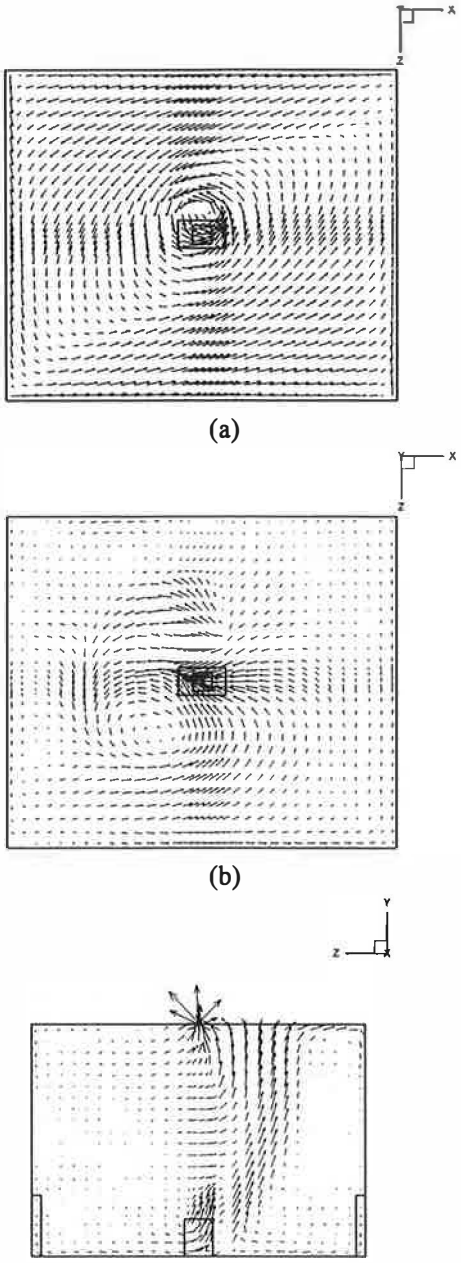

(a)

(b)

(c)

Figure 5 Velocity vectors at 30 min for Vortex Ventilation system seen from: (a) Above floor level, (b) Below ceiling level and (c) Midway along x-direction.

REFERENCES

Li, Y., Sandberg, M. and Fuchs, L. (1992) Vertical Temperature Profiles in Rooms Ventilated by Displacement: Full-Scale Measurement and Nodal Modelling. *Indoor Air*, 2, 225-243.

Orszag, S. A., Yakhot, V., Flannery, W. S., Boysan, F., Choudhury, D., Maruzewski, J. and Patel, B. (1993) Renormalization Group Modeling and Turbulence Simulations. *Near Wall Turbulent Flows*, Elsevier Science Publishers, New York.

Stone, H. L. (1968) Iterative Solution of Implicit Approximations of Multi-dimensional Partial Differential Equations. *J. Num. Analysis*, 5, 530-558. Van Doormal, J. P. and Raithby, G. D. (1984) Enhancements of the SIMPLE Method for Predicting Incompressible Fluid Flows, *Num. Heat Transfer*, 7, 147-163.

Yakhot, V. and Orszag, S. A. (1992) Development of Turbulence Models for Shear Flows by a Double Expansion Technique, *Phys. Fluids A*, 4, 1510-1520.